SPACE SHUTTLE ORBITER PN CODE SYNCHRONIZATION

Sam W. Houston
TRW Defense and Space Systems Group
Redondo Beach, California

ABSTRACT

The S-band Communications link to the Space Shuttle Orbiter from ground stations via TDRSS are transmitted spread spectrum to reduce the incident power flux density on the Earth's surface. This paper describes the requisite spread spectrum processing onboard Shuttle.

INTRODUCTION

S-band communications between the Space Shuttle Orbiter (SSO) and ground are relayed via the Tracking and Data Relay Satellite System (TDRSS) as shown in Figure 1. The maximum allowable power flux density on the Earth's surface is controlled by NASA and CCIR international agreement in accordance with the specification inserted in Figure 1. Staying within this power flux density limitation requires that the 96 kbps or 216 kbps PSK data be transmitted spread spectrum on the forward link. This is accomplished by a direct sequence psuedorandom noise (PN) code operating at 11.232 Mbps. The formation of the spread spectrum waveform is illustrated in Figure 2.

Prior to the ultimate demodulation of the 96/216 kbps data, the SSO receiver must "despread" the forward link waveform. This is accomplished by the SSO Spread Spectrum Processor (SSP) using the technique shown in the block diagram of Figure 3. A "replica" of the PN code is compared to that of the received waveform by a balanced modulator. The SSP acquisition circuitry searches for code alignment in 1/2 chip steps, dwelling at each code phase hypothesis for a predetermined decision interval. If the two code sequences are aligned to within a chip period a sinusoidal signal (PSK modulated) plus noise appears at the output of the balanced modulator. This output is continuously envelope detected and compared to a "noise-riding" threshold which announces the acquisition event. After acquisition the SSP enters the PN code tracking mode.

The remainder of this paper will briefly treat the fundamentals of the code acquisition analysis, the code phase tracking algorithm, and the key performance parameters of the completed unit.

CODE ACQUISITION ANALYSIS

The acquisition stage of synchronization ends with the local and received codes within 1/4 chip of coincidence. A second-order, early-late code tracking loop is then activated which pulls in and maintains code alignment.

The block diagram of the noncoherent acquisition circuitry of the spread spectrum receiver is shown in Figure 3. The local code from the onboard PN code generator is crosscorrelated with the incoming signal in the balanced modulator. If the two codes are in synchronism the output is a sinusoidal signal plus noise; otherwise the signal remains spread to a noise bandwidth $W \cong 2/T_c$, where T_c is the code chip duration. The correlator output is next bandpass-filtered to an IF bandwidth $B \ll W$ and noncoherently detected. After integration for time T, the signal is applied to a threshold device for a synchronization decision.

The time required to observe a given code phase, T, is determined by the predetection filter bandwidth, B, the input signal-noise-ratio, X, and the required detection and false alarm probabilities, Q_d and Q_o, respectively. For BT = 1, i.e., no post-detection integration, the probability density function (p.d.f.) of the detector output, Y, is Rayleigh if the signal is absent (i.e., X is noise only). Hence, the false alarm probability is given by

$$Q_o = \int_{\theta}^{\infty} \frac{V}{\sigma^2} e^{-V^2/2\sigma^2} dV \tag{1}$$

where

$$\theta = \text{threshold voltage}$$

$$\sigma^2 = N_oB = \text{input noise power}$$

If the input to the envelope detector (square-law device) is a sinusoid plus noise, the output p.d.f. is Rician. Hence, the probability of detection is

$$Q_d = \int_{\theta}^{\infty} \frac{V}{\sigma^2} \exp\left[\frac{-V^2-P^2}{2\sigma^2}\right] I_o\left(\frac{PV}{\sigma^2}\right) dV \tag{2}$$

where P is the amplitude that the sine wave would have at the output of the filter if noise were absent, and I_o is the modified Bessel function of the first kind. This is the Q-function

$$Q_d = Q\left(\frac{P}{\sqrt{2}\,\sigma}, \frac{\theta}{\sigma}\right) \tag{3}$$

as tabulated by J.I. Marcum.*

A good and useful approximation results for low input signal-to-noise ratios, X, requiring larger BT products to achieve practical detection and false alarm probabilities. For BT $\geq$ 10, the p.d.f.'s for both noise only and sinusoid plus noise approach Gaussian densities. The detection and false alarm probabilities may then be written as

$$Q_d = \phi[Y_s] = 1/2 \left[1 + \mathrm{erf}\left(\frac{Y_s}{\sqrt{2}}\right)\right] \tag{4}$$

and

$$Q_o = 1 - \phi[Y_n] = 1/2 \left[1 - \mathrm{erf}\left(\frac{Y_n}{\sqrt{2}}\right)\right] \tag{5}$$

where

$$Y_s = \frac{\mu_s - \theta}{\sigma_s} \tag{6}$$

$$Y_n = \frac{\theta - \mu_n}{\sigma_n} \tag{7}$$

and $\Phi[\cdot]$ is the standard normal distribution function. For purposes of evaluating (4) and (5), the moments of the Gaussian distributions may be written as

$$\mu_s = BT\,[1 + X] \tag{8}$$

$$\sigma_s^2 = BT\,[1 + 2X]$$

for the sinusoid plus noise case, and

$$\mu_n = \sigma_n^2 = BT \tag{9}$$

for the noise only case.

* "Table of Q Functions," J.I. Marcum, U.S. Air Force Project Rand Research Memo, January 1, 1950.

To determine dwell time, evaluate the error function arguments, Y_s and Y_n, in (4) and (5) for a desired Q_d and Q_o. Then equate the threshold value θ in (6) and (7). This yields the locus of predetection SNRs, Y, and BT products which achieve the desired probabilities of detection and false alarm.

PN CODE TRACKING LOOP

For tracking the SSP utilizes an early-late, delay-locked loop circuit. The block diagram of Figure 4 shows a non-time-shared punctual, early, and late tracking circuit implementation. Observe that the tracking error signal is obtained by detecting the energy at plus and minus 1/2 chip about the punctual code phase position. The RMS tracking error and approximate pull-in time is indicated in Figure 4. A relatively high single-sided loop bandwidth of 500 Hz is used for rapid acquisition and pull-in. The loop bandwidth is then reduced to 10 Hz for an improved tracking performance.

PERFORMANCE SUMMARY

The detailed block diagram of the SSP is shown in Figure 5. The IF input enters a three-way power divider to allow the paralled PN code acquisition, tracking, and despreading operations. Switchable bandpass filters accommodate both 96 or 216 kbps data.

Acquisition time is a primary figure-of-merit. Shown in Figure 6 are the test measurements, over temperature and in the presence of doppler, of the 0.99 probability time to acquire versus carrier-to-noise density for the 96 kbps data. The key performance parameters of the SSP are summarized in Table 1.

TABLE 1. SUMMARY OF SSP PERFORMANCE

PN CODE RATE	11.232 MEGACHIPS/SEC
PN CODE LENGTH	2047 CHIPS
PN MODULATION	PSK/NRZ
DATA RATES	96/216 KBPS
DATA MODULATION	PSK/MANCHESTER
INPUT SNR (IN SPREAD BANDWIDTH)	-25.5/-22.0 DB
CODE DOPPLER	±100 HZ
0.99 PROBABILITY ACQ TIME	12.7/3.1 SEC
ACQUISITION B_L	500 HZ (SINGLE-SIDED)
TRACKING B_L	10 HZ (SINGLE-SIDED)
PULL-IN TIME	79.3 MSEC
RMS TRACKING ERROR	0.056 CHIP
PROB OF LOSS-OF-LOCK	$< 10^{-4}$ (IN TEN HOURS)

The paper concludes with a photograph of the SSP, shown in Figure 7, assembled and ready for installation in the SSO network transponder. The unit houses the complete acquisition and tracking circuitry, the RF equipment, and the digital equipment, each on separate layer boards.

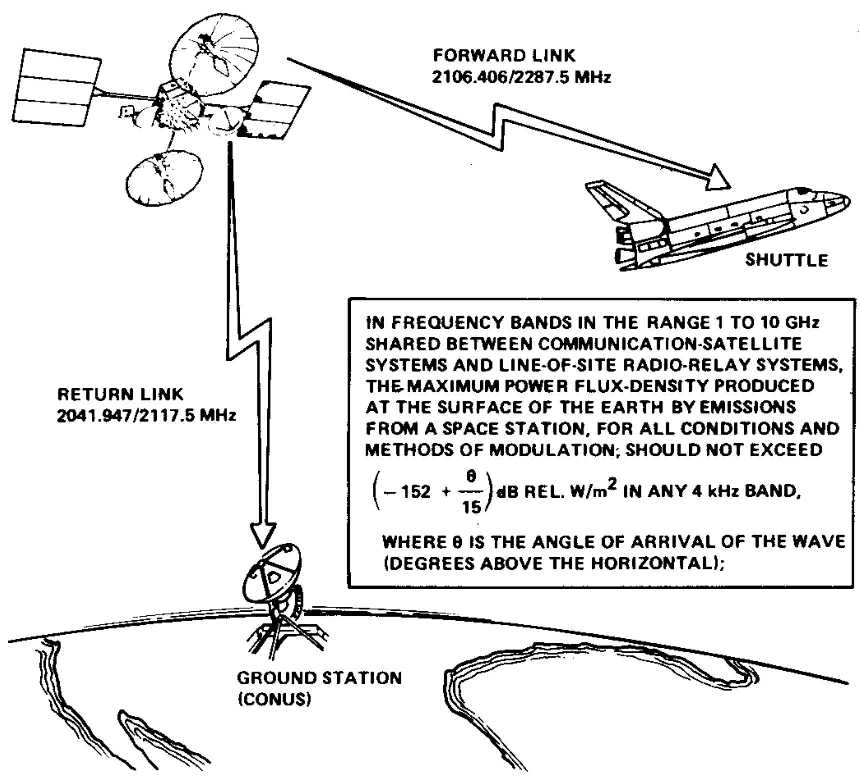

Figure 1. Shuttle/TDRSS NASA S-Band Communication Links

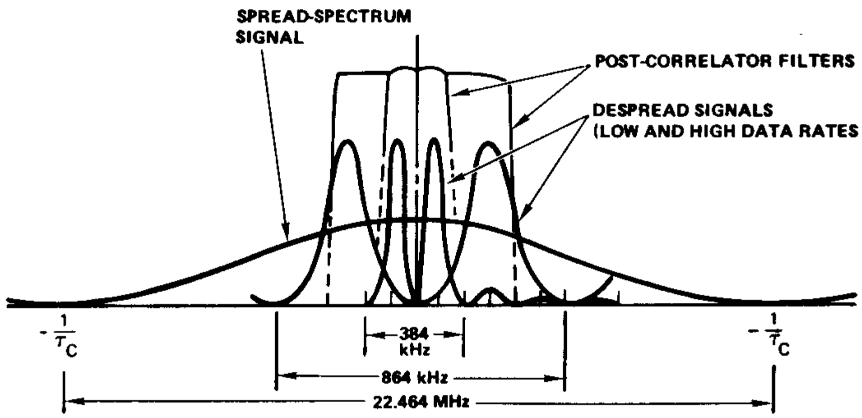

MANCHESTER PSK BASEBAND MODULATION:

$$v(t) = A \cos \omega_c t + \phi_{PSK}(t) \qquad \phi_{PSK} = \pm \pi/2$$

PSEUDORANDOM NOISE (PN) DIRECT SEQUENCE CODE PHASE MODULATION:

$$\begin{aligned} v(t) &= A \cos \omega_c t + \phi_{PSK}(t) + \Theta_{PN}(t) \\ &= A \cos \Theta_{PN}(t) \cos\left[\omega_c t + \phi_{PSK}(t)\right] \\ &= A\, p(t) \cos\left[\omega_c t + \phi_{PSK}(t)\right] \end{aligned}$$

P (t) TAKES VALUES ± 1 EVERY τ_c SECONDS, AT "RANDOM"

Figure 2. Formation of the Spread Spectrum Waveform

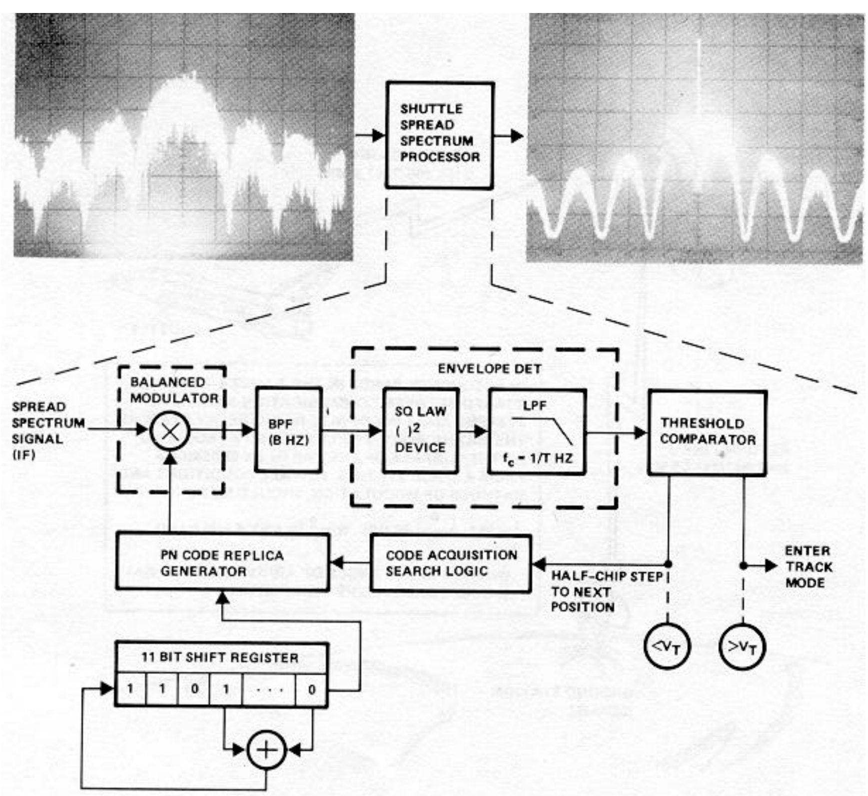

Figure 3. Despreading Function of SSP

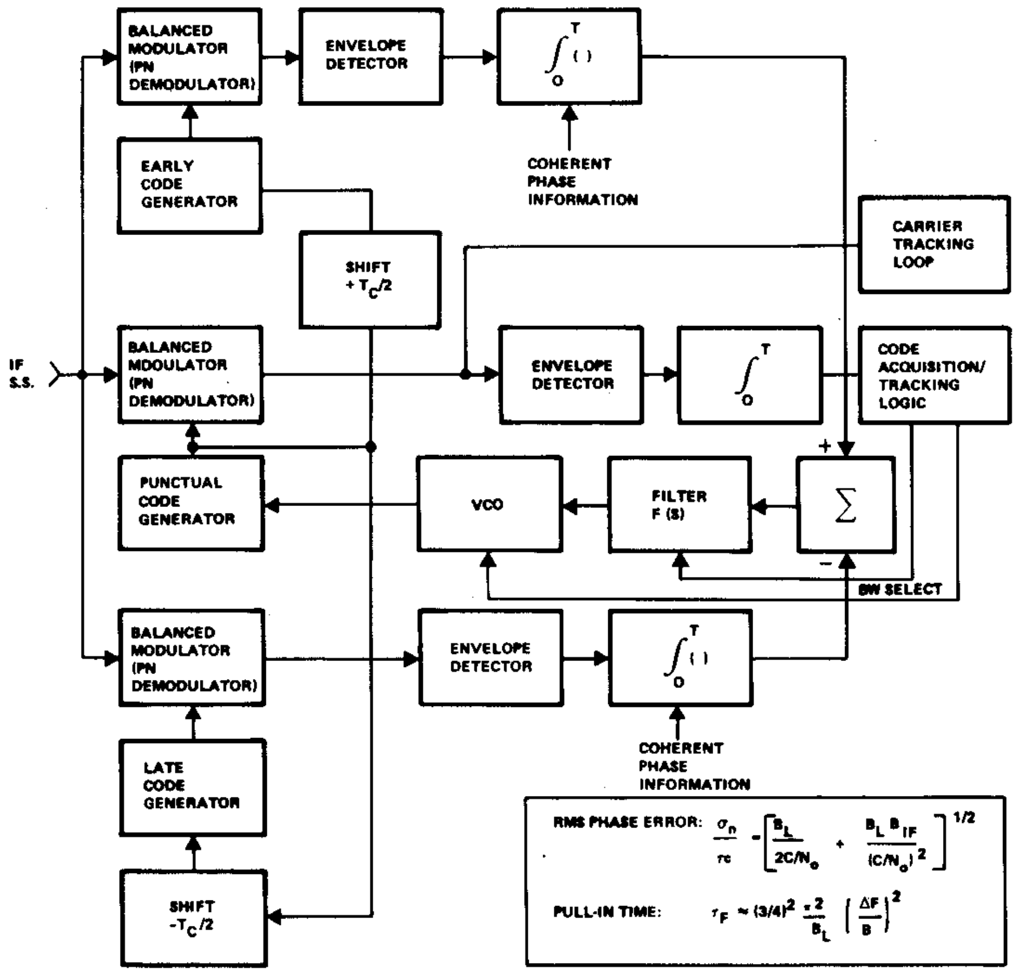

Figure 4. Early-Late Delay Locked Loop

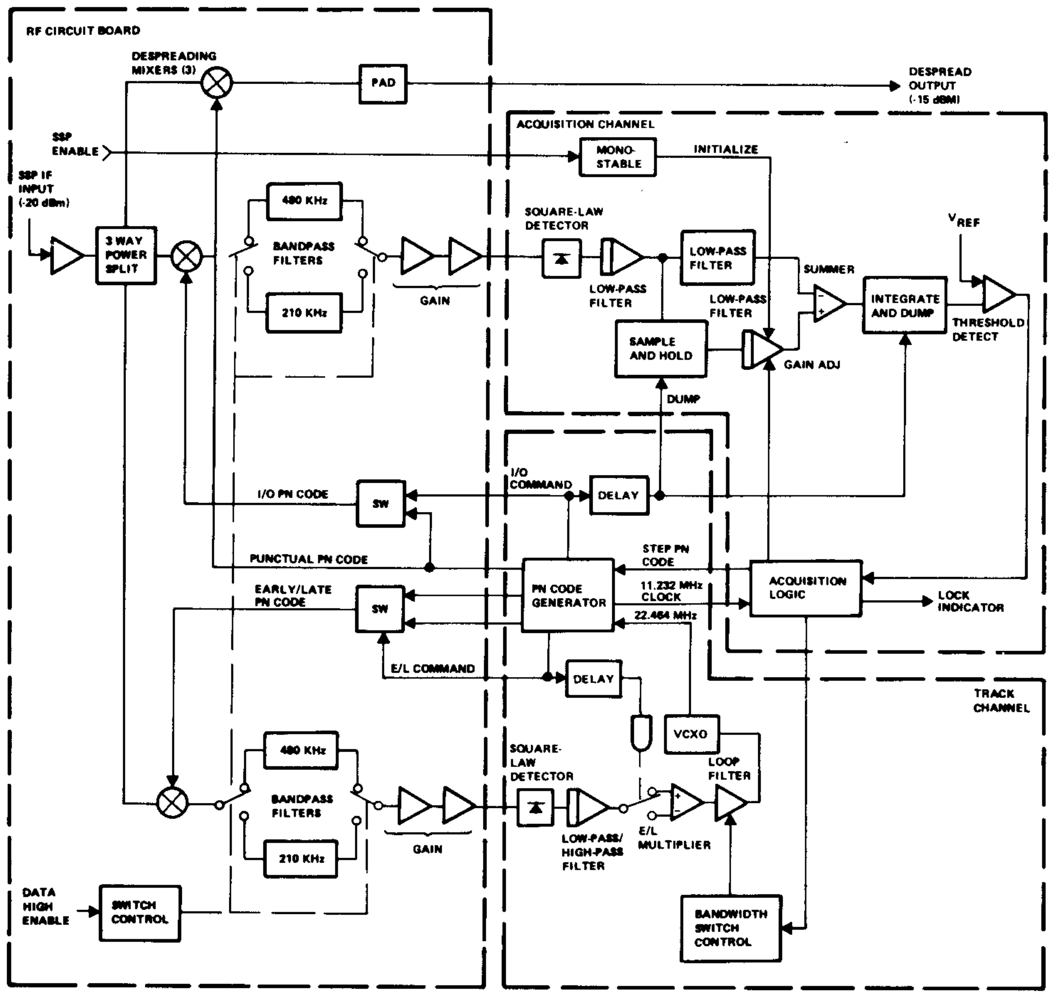

Figure 5. Spread Spectrum Processor Block Diagram

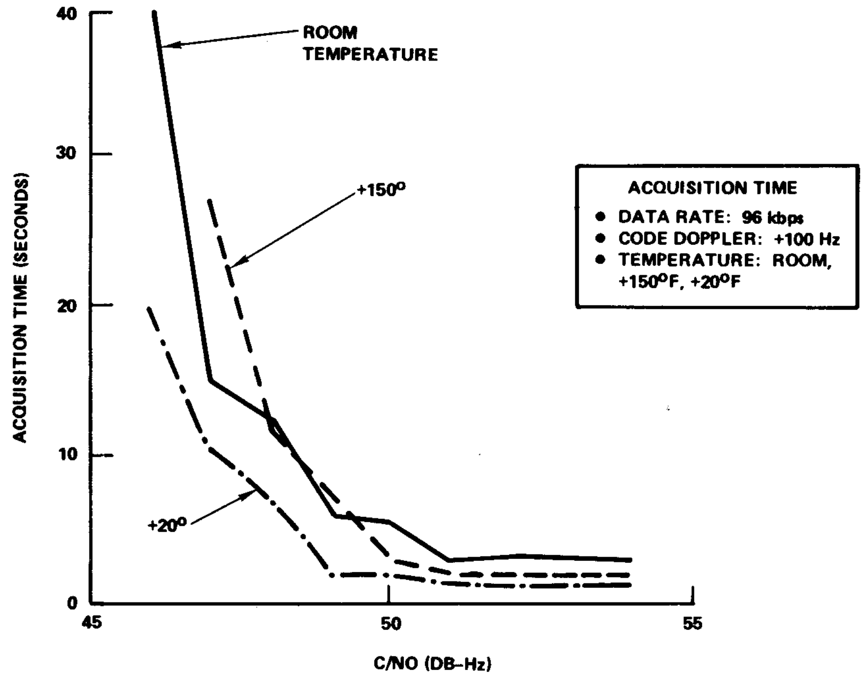

Figure 6. Shuttle Test Data

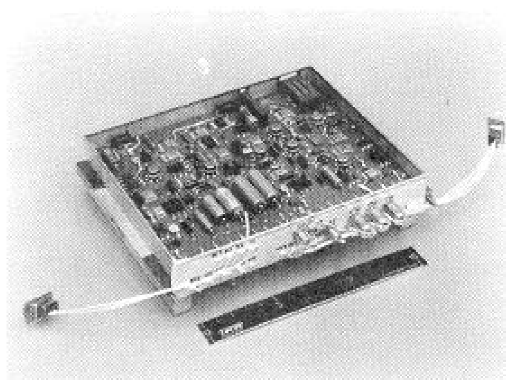

Figure 7. Shuttle Spread Spectrum Processor